THE PENNSYLVANIA STATE UNIVERSITY
SCHREYER HONORS COLLEGE

DEPARTMENT OF CHEMICAL ENGINEERING

LOW TEMPERATURE HIGH PRESSURE ADSORPTION OF NITROGEN BY RPM3-ZN USING A DIFFERENTIAL PRESSURE ADSORPTION UNIT

ANDREW BELNICK
SPRING 2016

A thesis
submitted in partial fulfillment
of the requirements
for a baccalaureate degree
in Chemical Engineering
with honors in Chemical Engineering

Reviewed and approved* by the following:

Angela Lueking
Associate Professor of Energy and Mineral Engineering and Chemical Engineering
Thesis Supervisor

Michael Janik
Professor of Chemical Engineering
Honors Adviser

* Signatures are on file in the Schreyer Honors College.

ABSTRACT

Adsorption as a method of separating air is highly preferable over other processes like cryogenic distillation due to the lower cost of utilities and more moderate temperature and pressure conditions. Metal organic framework materials are a promising way to accomplish this separation of nitrogen and oxygen. One of which is RPM3-Zn, a material synthesized and tested by collaborators at Rutgers University. This material warrants further research, as preliminary data has shown it to be selective to oxygen over nitrogen at low temperature. Because the molar ratio of oxygen to nitrogen is nearly 1:4, a company needs only a quarter of the material and process utilities for an oxygen selective MOF over a nitrogen selective MOF. Experiments were conducted using this material and nitrogen gas at 195K and 20 bar/65 bar. They were completed on a custom differential pressure adsorption unit built by Dr. Angela Lueking at Penn State University. Helium was used as the blank non-adsorbing gas differential pressure correction. The sample cells were maintained at 195K using a bath of acetone and dry ice. All experiments were run for 16 hours. Extreme fluctuations in dP with time were observed and thought to be a function of changes in the temperature in the room as well as changes in the height of the temperature bath. Consequently, only the first 2 hours of data were used in determining the moles of nitrogen adsorbed. Similar fluctuations in dP with time were observed in the helium blank experiments. In the 20 bar experiments 0.540 and 0.854 mmol N_2/g RPM3-Zn were observed and in the 65 bar experiments 1.222 and 0.711 mmol N_2/g were observed. This is close to the value of 1.8 mmol/g found on the IGA for 195K/ 20 bar, with the deviation likely due to problems in controlling temperature and possible contamination of the sample.

TABLE OF CONTENTS

LIST OF FIGURES

LIST OF TABLES

ACKNOWLEDGEMENTS

Special thanks to Dr. Lueking for allowing me to work in her lab and complete this project. I am so grateful for her patience, wisdom, and expertise in this research area. I would not have gotten off the ground without her. Thanks to the Dr. Jing Li at Rutgers University for the samples to use for this project. Thanks to my parents, family, and friends for their support. The last four years have been a roller coaster and I would not have made it without them.

Chapter 1 Literature Review and Statement of Purpose

Statement of Purpose

The separation of air into its constituent gases is a multibillion-dollar industry and so it is critically important to understand the most energy and cost effective way to accomplish this process. One such way to do so is by an adsorption process where a material can selectively adsorb nitrogen or oxygen from a stream of air, from which the purified gas can later be desorbed and captured. The amount of gas captured depends of a wide number of system and material properties, including but not limited to temperature and pressure of the adsorption system. In general, for physical adsorption, as temperature decreases and pressure increases the capacity of the adsorbent is expected to increase. However, at extremely low temperatures or high pressures physical adsorption will likely not be economically viable. Desirable physical adsorbents would operate at near ambient temperatures and moderate pressure. Ideally, they would have a large molar adsorption of gas for a small pressure increase.

A custom differential pressure system designed and built by Dr. Angela Lueking works by determining the differential pressure between a cell with an active adsorbent on one side and a non-adsorbing ballast material on the other in the presence of a gas. The moles of gas can be determined from the differential pressure created between the two sample cells. The goals of this project were twofold. The first was to develop a methodology for conducting low temperature adsorption measurements with this differential pressure system, as this has not been attempted on this equipment in Dr. Angela Lueking's lab.

The second goal was to further understand the high oxygen selectivity of a particular material, RPM3-Zn. Oxygen selectivity is defined as a material's ability to preferentially adsorb

oxygen over other gases from a gas mixture such as air. RPM3-Zn is a metal organic framework (MOF) material developed by researchers at Rutgers University and will be discussed further in Chapter 3. Preliminary data has shown that this material selectively adsorbs oxygen over nitrogen. The overarching direction of this research project is to develop a material that preferentially adsorbs oxygen at room temperature; using such a MOF to extract oxygen from air would require a fourth of the energy and material over a nitrogen selective MOF, as the ratio of nitrogen to oxygen in air is approximately 4:1 [7]. The result is a significant decrease in the amount of energy and adsorbent required to purify air with an adsorption process.

This work looked at the moles of nitrogen adsorbed to RPM3-Zn at 195K and both 20 bar and 65 bar. The operating equation for determining moles of gas adsorbed was modified to include a temperature correction parameter (τ_A) to account for the temperature gradient between the sample cells and the upper subsystem of the differential pressure unit. Although low temperature experiments are standard on traditional adsorption equipment that measures adsorption at 77K up to 1 bar, this is less common for high pressure adsorption measurements. The intent was to also compare the adsorption equilibrium to experiments conducted at 195K on a gravimetric gas sorption analyzer. The temperature gradient between the sample cells and upper subsystem was maintained as constant as possible, though the effects of the heat of adsorption and evaporation of acetone in the cold bath may have caused the τ_A parameter to fluctuate. This is explored further in Chapter 5 Results and Discussion.

Economics of Separation of Air

Air is composed of 78.084% nitrogen, 20.947% oxygen, 0.934% argon by volume, with trace amounts of carbon dioxide, neon, helium, methane, krypton, hydrogen, etc. making up the remainder [1]. There is a market for each of these gases in their pure form, thus the separation of

air into these constituents represents a significant business opportunity. According to the IHS Chemical Economics Handbook for Air Separation Gases, the market is controlled by four major global companies who together supplies 60 – 70% of these products. These companies are Air Products and Chemicals Inc. (United States), L'Air Liquide (France), The Linde Group PLC (United Kingdom), and Praxair Inc. (United States) [2].

Demand for both industrial oxygen and nitrogen is expected to mostly increase through 2018 in the four major industrialized regions of the world. Specifically, the demand for oxygen is expected to increase over 200 thousand metrics tons/day through 2023 as the demand for clean energy increases. The expected percent increase in demand for nitrogen and oxygen are summarized in Table 1 below. Note that this table only account for increases in oxygen and nitrogen demand for industrial processes and does not include the increase in demand for oxygen for use in oxy-combustion. Oxy-combustion is the process where oxygen, rather than air, is used as the oxidant in combustion processes. Doing so reduces fuel consumption because nitrogen, which is not chemically consumed during combustion, does not need to be heated. The increase in oxy-combustion technology, too, will contribute to an increase in the demand for oxygen[9].

Table 1. Increase in consumption of oxygen and nitrogen by region of the world from 2013 through 2018 (in millions of cubic meters)[2].

	Oxygen	Nitrogen
United States	3.10%	4.20%
EMEA	2.80%	2.30%
Japan	-0.03%	0.00%
China	6.40%	4.10%

These gases are used across a wide number of manufacturing operations including chemical synthesis and processing, primary metal and fabricated metal products, oil and gas extraction, petroleum refining, food processing, and glass manufacturing. Figure 1 below shows

a breakdown of which industries are using industrial nitrogen and oxygen. Note that primary metal production makes up over a third of industrial oxygen consumption and bulk chemical production makes up over a third of industrial nitrogen consumption.

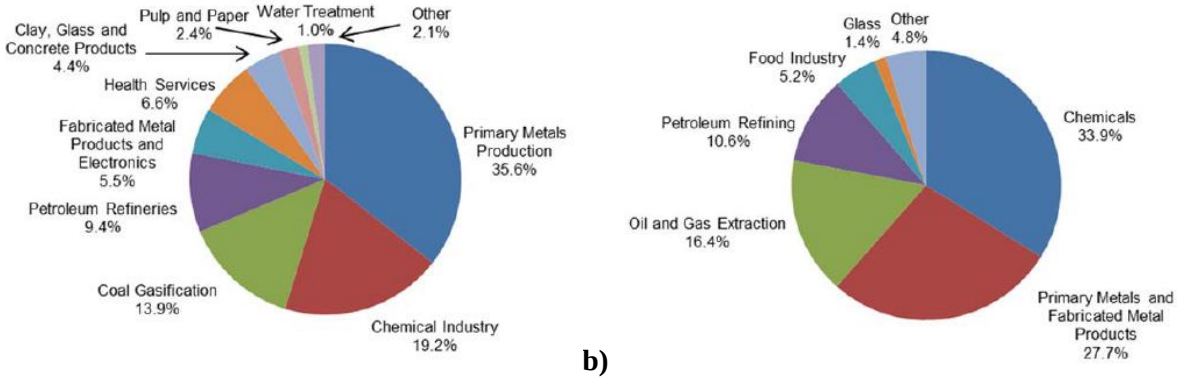

a) **b)**

Figure 1 a. Consumption of oxygen by industry in the United States in 2013. Total consumption was 18.8 billion cubic meters b. Consumption of nitrogen by industry in the United States in 2013. Total consumption was 23.7 billion cubic meters[2].

The cost of separating these gases from air depends on the level of purity and quantity demanded, as different technologies for separating air become more or less economical based on these parameters. Figure 2 below shows the regions where membrane separation, pressure swing adsorption and cryogenic distillation are the most economical for delivering pure oxygen. The IHS Chemical Economics Handbook reports adsorption is most economical when 1 – 500 tons/day of oxygen are required between a purity of 80% - 93%. Cryogenic distillation for oxygen is most economical when high purity is required, on the scale of 93% to 100% [2]. It is also most economical when a large volume is required at a near constant rate, about 500 – 1000 tons/day[2]. Cryogenic distillation is expensive for low demand due mainly to the electricity costs of cooling air to a liquid form for distillation, encompassing 40 – 70% of the cost to operate the unit[2]. As a result, it is clear that research into oxygen-selective MOFs is timely and may eventually be competitive with cryogenic distillation for all purities and daily demands.

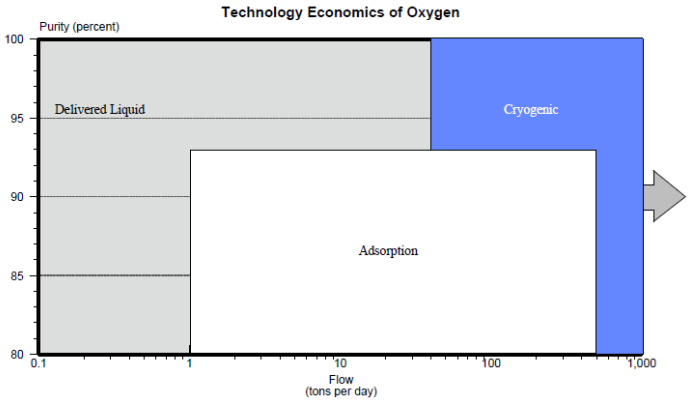

Figure 2. Oxygen purity v. required oxygen flow rate. This graph shows which technology is the most cost effective for a given purity required and flow rate[2].

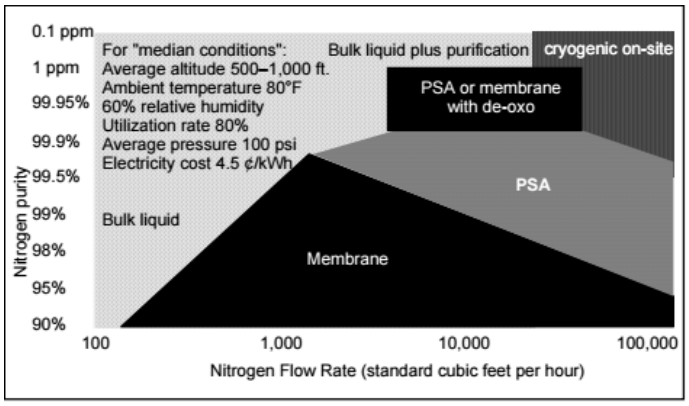

Source: Thomas Hardenburger, "Producing Nitrogen at the Point of Use," *Chemical Engineering*, October 1992, p. 146.

Figure 3. Nitrogen purity v. required nitrogen flow rate. This graph shows which technology is the most cost effective for a given purity and flow rate[2].

Metal Organic Framework Materials

Metal organic frameworks (MOFs), or porous coordination polymers (PCPs), represent one of the most promising materials for separating gas mixtures and capturing certain gases out of air and flue gas[4]. The sample used for these experiments was synthesized by collaborators at Rutgers University from the Dr. Jing Li's Group. It is from a new class of microporous metal organic framework materials being developed at Rutgers under the name RPMs (Rutgers Recyclable Porous Materials). The specific material used for this experiment was

$Zn_2(bpdc)_2(bpee)$; bpdc = 4,4'-biphenyldicarboxylate; bpee = 1,2-bipyridylethene which henceforth will be called **RPM3-Zn** [6].

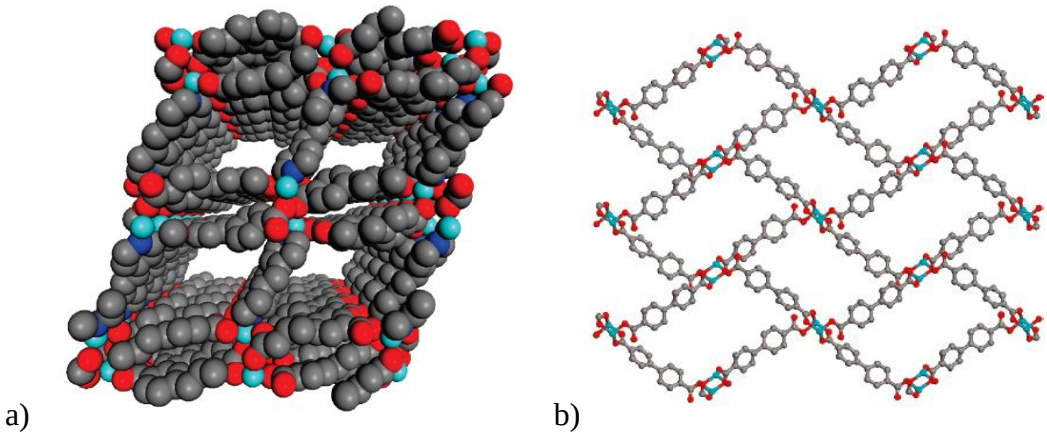

a) b)

Figure 4. a) Computer rendering of RPM3-Zn; Aqua = Zn, Gray = C, Red = O, Blue = N. b) Single layer of coordinated atoms of the metal organic framework[6].

According to previous reports, the sample has a ship-and-bottle structure, where the bottle is the tube-like structure evident in the figure above[6]. The tubes are approximately 5x7 Å. The channel is wide enough to allow 2 diatomic hydrogen molecules to adsorb at the same time, thus a unit cell of this material can accommodate 16 diatomic hydrogen molecules. The ship represents the product gas that is being adsorbed and bonding with the internal structure of the material. This particular material can break down by being placed in water. The material was shown to adsorb 4.97 wt. % nitrogen at room temperature and 70 bar[6].

This material was also shown to have gate-opening properties. Gate-opening materials generate an unusual S-shaped adsorption profile; the material has a closed structure and minimal adsorption at low pressures but above a specific pressure, the structure opens to allow for guest gas molecules. This pressure is designated P_{GO} and is dependent on the temperature and gas molecule being adsorbed, among other factors[10].

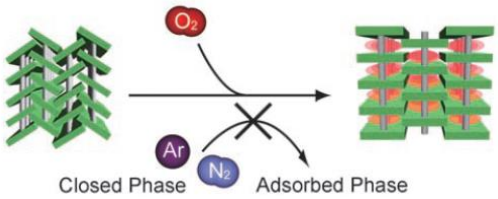

Figure 5. Structure of a gate-opening material above and below P_{GO}[10].

Low Temperature Adsorption and Previous Data

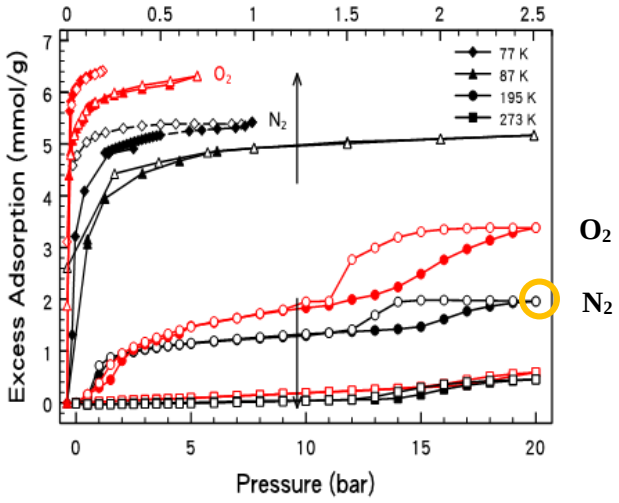

Figure 6. Preliminary data from Dr. Angela Lueking at Penn State University and Dr. Jing Li at Rutgers University showing the oxygen selectivity of RPM3-Zn at different temperatures. O_2 data is show in red and N_2 data is shown in black[7].

The reason that RPM3-Zn was chosen to investigate further was because of preliminary data that shows that it is oxygen selective at a wide range of temperatures. The benefits of an oxygen selective material have already been discussed. As seen in Figure 6, at all of the temperatures studied (77K, 87K, 195K. and 273K) the oxygen isotherm is above the nitrogen isotherm meaning more oxygen is adsorbed than nitrogen at a given temperature. It should also be noted that at lower temperatures the difference in nitrogen adsorption to oxygen adsorption is more exaggerated. One set of experimental conditions of this thesis are nitrogen at 195K and 20 bar; the excess adsorption as found in this experiment was 1.8 mmol/g, circled in orange in

Figure 6[7]. Experiments at 195K are particularly interesting because prior work suggests that a shift in the diffusion rate between N_2 and O_2 occurs at this temperature and at multiple different pressures[7]. Below this temperature, N_2 diffuses slower than O_2 because this molecule takes longer to open the GO-MOF structure. Above this temperature, it was found that N_2 diffuses more quickly than O_2[7]. This project may help to clarify what change, structural or chemically, is occurring in this temperature regime.

The novelty of this project is that the experiments conducted with the differential pressure adsorption system were done at high pressure and 195K instead of room temperature. Moreover, previous work at 195K was limited to experiments with pressure below 20 bar. Low temperature experiments have not been studied in detail on the differential pressure adsorption system before and thus the operating equations used to determine moles of adsorbed gas at room temperature were not adequate. Low temperature adsorption experiments are easily accomplished on traditional and commercially available instruments, like Micromeritics Accelerated Surface Area and Porosimetry System 2020 which is also used in this lab. However, this equipment is limited to a maximum pressure of one bar. The operating equation used by this machine is discussed in Chapter 4 Calibrations.

Chapter 2 Differential Pressure Adsorption System

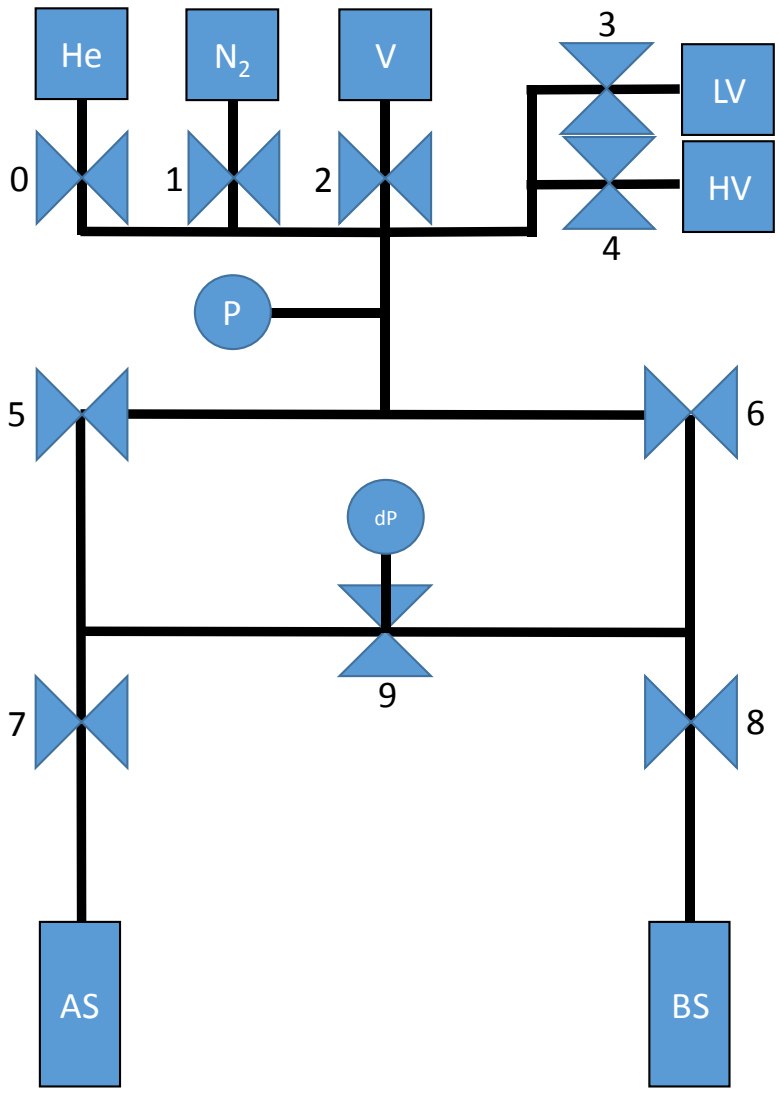

He – Helium inlet from cylinder

N_2 – Nitrogen inlet from cylinder

V – Vents system to external relief

LV – Pulls low vacuum

HV – Pulls high vacuum

P – Absolute pressure transducer

dP – Differential pressure transducer

AS – Cell for adsorption sample

BS – Cell for nonadsorbing inert sample.

Figure 7. Differential pressure system schematic including valves and transducers

The differential pressure system diagramed above was used for all experiments. It was designed and built by Dr. Angela Lueking at Penn State University[8]. In adsorption experiments one of the main sources of error is in determining the absolute pressure change in the system as the adsorbent is exposed to a gas and this is exacerbated at high pressure due to the relative error in the pressure measurement. The main rationale for building this system was that by using a

differential pressure transducer the measurement taken would be upwards of 10-fold smaller than the measurement an absolute transducer would make during the experiment. As accuracy is proportional to the magnitude of the measurement, a 10-fold reduction in the measurement made results in a 10-fold increase in the accuracy of that measurement[8]. It was found that operating equations and methods developed around this differential pressure system could decrease sensitivity to volume uncertainties 300-fold[8]. These operating equations are discussed in Chapter 3 Methods.

The system is set up to be an approximate mirror image. The left side, where one of the cells is labeled AS, is the sample cell of the adsorbent material to be tested. The right side, where one of the cells is labeled BS, is the sample cell of a blank non-adsorbing material. The operating principle of the equipment is that the blank sample will not adsorb any gas. As the active sample on the A side of the system adsorbs gas, a differential pressure is created and from that differential pressure, along with the temperature correction parameter, volume of the subsystem components, and dP data from helium blank experiments, the moles of adsorbed gas can be determined and plotted from a derived operating equation. Note that to get a 'true' mirror image a ballast would need to be added with the exact volume of the adsorbent sample. As this is difficult and introduces the potential for systematic error, asymmetries are handled mathematically[8].

The system uses ¼" stainless steel tubing with compression fittings throughout, with pneumatic vales that are controlled through a LabView program (v 7.1). The system contains two gas inlet lines set up for an adsorbent gas and helium. Helium is non-adsorbing and used for pressure calibration, volume calibration, and temperature correction parameter experiments. Nitrogen (Ultra High Purity grade, 99.999%) was used for the adsorption experiments. There is

also an external vent line to vent the system after each experiment. Valves 3 and 4 control the vacuum pump lines. A BOC Edwards XDS5 vacuum pump is used for this system. There are two levels, low vacuum pulls down to 0.05 bar and the high vacuum pulls down to 0.01 bar.

There are two pressure transducers in the system (labeled P and dP in the diagram above). The absolute pressure transducer has a limit of 100 bar (± 0.05 bar) and the differential pressure transducer has a limit of 6.9 bar (± 0.01 bar). The absolute pressure transducer is in the manifold section of the system and the differential pressure transducer provides the boundary between subsystems.

Valves 5,6,7,8, and 9 define and restrict access to different parts of the system. The subsystem formed when 5,6,7,8, and 9 are closed is called the upper manifold. The subsystem bounded by valves 5,7, and 9 is called Va. The subsystem bounded by 6,8, and 9 is called Vb. The subsystem below valve 7 is called Vas. The subsystem below valve 8 is called Vbs. Vaas and Vbbs will also be used; Vaas refers to the subsystem bounded by 5 and 9 with 7 open while Vbbs refers to the subsystem bounded by 6 and 9 with 8 open. From this point forward, these subsystem names will be used.

Chapter 3 Methods

Leak Testing: Because experiments of this type hinge on a leak-free system for accurate measurements, a leak test was performed on the system before experimentation began. The entire system was charged and held with helium at 80 bar and the P and dP were monitored. There was no fluctuation in dP, the more sensitive of the measurements between P and dP. Also, a Hiden Analytical DSMS Mass Spectrometer was used to detect helium leaks. No leaks were detected by the mass spectrometer at any of the valves, joints, or connections.

Volume and Pressure Calibration: Volume and pressure calibrations were performed on the system using helium before experimentation began. Reference Chapter 4 Calibrations for procedures and data about how pressure, volume, and the temperature correction parameters were calibrated for the differential pressure system.

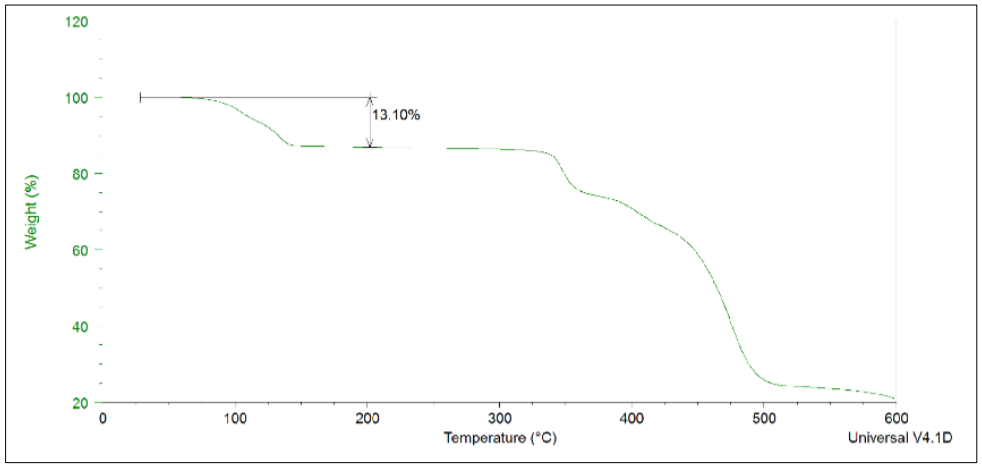

Figure 8. Thermogravimetric analysis of RPM-3-Zn[6].

Degassing/Drying: Figure 8 shows the thermogravimetric analysis conducted by collaborators at Rutgers University; it indicates that this sample is guest-free when heated between 150°C and 350°C. At temperatures below this solvent remains in the material and at temperatures above this the sample begins to degrade. As a result, a degassing procedure of 10 hrs at 135°C was

suggested by Dr. Jing Li at Rutgers University. For the initial solvent removal, the sample was loaded into a long stem glass bulb cell and degassed on a Micromeritics ASAP 2020 Plus Physisoption unit. The program that was used was an increase of 0.5°C from room temperature to 135°C and then held at this temperature for 10 hours.

The sample was then cooled to 298K and transferred to an adsorption cell consisting of a double-male VCR coupling of 5 ± 0.05 cc sealed with a 0.5 μm gasket filter. The weight of this fixture empty and then with the sample is taken to determine the weight of the degassed sample. 84.1 mg of sample RPM3-Zn was used. Both cells were attached as shown in Figure 7 and the vacuum pump was used to reduce the pressure to 0.01 bar. The sample was heated using a temperature microcontroller process unit at 150°C for 8 hrs to desorb any adsorbed gas or residual solvent by fitting heated jackets around the entire sample cell. Heat tape was also wrapped around the tubing between the system and sample cells. After 8 hrs the microcontroller and heat tape were removed and the sample was cooled under vacuum.

The adsorption sequence and control of the system was maintained through a LabView program that mimics the actual equipment set up. A screen capture of the LabView program is shown below.

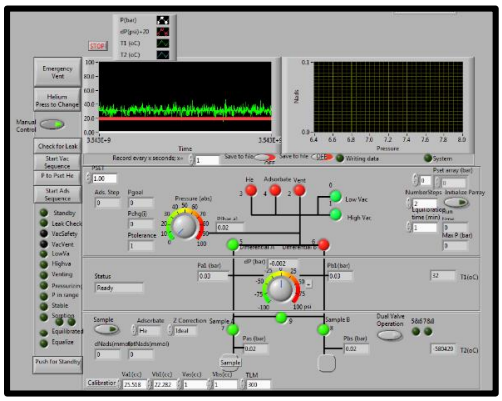

Figure 9. Labview control panel with location of valves and pressure control.

A dry ice and acetone bath was prepared to maintain the samples at 195K[12]. The dry ice was packed into a dewar and then raised to cover both sample cells. Acetone was poured into the dewar and allowed to equilibrate to the temperature of the dry ice. The temperature of the bath was monitored with a thermocouple during the course of the adsorption experiment. Acetone was filled to 1" below the top of the dewar at the start of the experiment. The dewar was then enclosed in an insulated bag. The sample cells and bath were allowed to thermally equilibrate for approximately 15 minutes.

Nitrogen gas was then charged to the system with valves 7 and 8 shut. This isolates the samples from the rest of the system. The PV relation of the ideal gas law was used to estimate the required charge pressure to Va to get a desired final pressure in the Vaas subsystem. The system pressure is read off the absolute pressure transducer.

$$\boldsymbol{P_{Charge} = \frac{V_{aas}}{V_a} * P_{Final}} \qquad \mathbf{1}$$

After charging, valves 5 and 6 are both shut. The system is allowed to thermally equilibrate for 15 minutes. Then, valve 9 is closed to isolate the sample side from the non-absorbing blank side. The system is again permitted to thermally equilibrate for 15 minutes. The initial differential pressure is recorded and data is saved to a file from this point. After the system has equilibrated valves 7 and 8 are opened to expose the samples to the charged gas. The system records the differential pressure between the sample and non-adsorbing blank side every second. It also records the thermocouple reading of the dry ice/acetone bath. Adsorption data was recorded for 16 hours before the adsorption experiment was terminated.

The final pressure in Vaa was determined by lowering the pressure in the manifold to approximately the pressure expected in Vaas with vales 5, 6, 7, and 8 closed. Valve 6 was then

opened and the pressure in Vaas could be determined based on the dP reading. The system was then evacuated and the sample degassed for another trial. The final level of the dry ice/acetone bath was recorded as well.

To determine the moles of adsorbed gas, a reduced volume of the adsorbing side (A) of the unit was defined as

$$\boldsymbol{\nu_{AAS} = \frac{V_A + V_{AS} + V_V}{Z_{RT} R T_{RT}}} \qquad \mathbf{2}$$

where V_A, V_{AS}, and V_V are volumes of those respective systems as discussed in Chapter 2, Z_{RT} is the compressibility factor at the given conditions, R is the gas constant, and T_{RT} is the room temperature.

Equation 3 is the operating equation used for determining the moles of adsorbed gas and is derived in the literature[8],

$$\boldsymbol{dN_{ads} = \nu_{AAS}^{TC} \Delta dP^{BC}} \qquad \mathbf{3}$$

where dN_{ads} is the moles of gas adsorbed by the material, $v_{AAS}{}^{TC}$ is the corrected reduced volume at the experimental temperature, and ΔdP^{BC} is the difference between the steady state differential pressure in the nitrogen and helium experiments. It can also be written as

$$\mathbf{dN_{ads} = \tau_A \nu_{AAS} (dP - dP^{He})} \qquad \mathbf{4}$$

where τ_A is the temperature correction discussed in Chapter 4 Calibrations, v_{AAS} is the reduced volume at room temperature, dP is the steady state differential pressure in the nitrogen experiment, and dP^{He} is the steady state differential pressure in the helium experiment. The nitrogen and helium experiments were completed at the same charge pressure.

Chapter 4 Calibrations

Pressure Calibration

Before any experiments could be run the pressure transducer and differential pressure transducer were calibrated. The transducers produce an electric signal in milliamps and that signal must be translated into a pressure. A series of experiments were run where helium was charged to the system up to a known pressure and the electrical signal as shown by LabView was recorded. A linear correlation between the actual pressure of the system and the electrical reading in milliamps was determined using least squares regression and Solver in Excel.

Procedure, Pressure Gauge: An external pressure gauge was placed on the sample B port so that an external pressure reading could be taken and calibrated to the system. The system was charged with helium up to a given pressure and the reading on the gauge was recorded as well as the electrical signal. This was done across the full range of the pressure transducer (0-100 bar). The data was then fitted to a linear model in Excel and least squares regression used to determine the appropriate m and b parameters that would translate a raw electronic impulse into the correct pressure reading.

Table 2. Sum Squared Regression for Pressure Transducer

Reading, mA	P_gauge (psi)	P_gauge (bar)	P_gauge_model (bar)	Error
0.005	92.3	6.366	6.4	0.00035
0.00477	71.8	4.952	4.9	0.00037
0.00431	29.6	2.041	2.0	0.00017
0.00409	9.1	0.628	0.6	0.00014
0.00453	49.6	3.421	3.4	1.2E-05
0.00415	14.7	1.014	1.0	2.1E-05
			Sum Sq. Error =	0.00107

Table 3. Parameters as Determined from Least Squares Regression

m	**6312.884**
b	**-25.180**

$$\boldsymbol{P_{LabView} = m * Reading\ [mA] + b} \qquad \textbf{5}$$

Procedure, Differential Pressure Transducer: The differential pressure gauge was calibrated in a similar fashion to the absolute pressure transducer. Va was charged to a given pressure with helium. The correct pressure could now be read off of the LabView output because the parameters determined above were inputted to the system. Va was then isolated by closing valves 5 and 9. The pressure in Va was known from the LabView reading before isolation. Additional helium was then charged to the system to create a differential pressure across the transducer. The pressure after this additional charge was recorded and the true differential pressure could then be determined. The electrical impulse for this differential pressure was also recorded. After each reading the system was vented except for Va. The system could then be charged again to observe another dP and corresponding electrical impulse. Experiments were run with Va charged to 0.1 bar, 1.05 bar, and 2.3 bar. In this way the calibration parameters for the differential pressure transducer were determined.

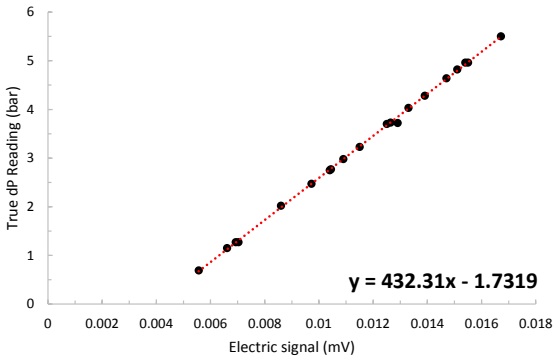

Figure 10. Determining the calibration parameters for the differential pressure transducer using true measurements

Table 4. Parameters as Determined by Least Squares Regression

m	**432.31**
b	**-1.7319**

Volume Calibration

The volume of the entire system, as well as the volume between each of the valves, had to be determined before any experiments were done. This was found by expanding a known volume of helium into a system with an unknown volume and reading the resulting change in pressure from the unknown system to the final. In summary, a gas is charged to the system which contains a reference cylinder of known volume. The reference cylinder was attached by removing the vent line above valve 3. The cylinder is charged to a known pressure and isolated from the remainder of the system with a pneumatic valve; the pressure of the gas in the cylinder is recorded. The system pressure is then vented by an arbitrary amount to create a pressure differential between the gas in the reference cylinder and the unknown system. The pressure of the system in this condition is also recorded. The gas in the cylinder is then expanded into the system of unknown volume and the final pressure is recorded. From these measurements the volume of the unknown system could be determined.

The derivation below shows how the volume of a given part of the system can be determined from the pressures of the reference volume, unknown system, and final pressure. The subscript R refers to properties of the reference volume, the subscript U refers to properties of the unknown system, the subscript F refers to properties of the final system, and the subscript V refers to properties of the valve. The internal volume of the valve used in the reference volume was determined from the manufacturers catalog.

Starting with a mole balance on the inert gas:

$$\boldsymbol{n_U + n_R = n_F} \qquad \textbf{6}$$

where n_U is moles of gas in the unknown system, n_R is moles of gas in the reference volume and n_F is moles of gas in the final combined system after expansion. With the ideal gas equation of state,

$$\frac{\boldsymbol{P_U V_U}}{\boldsymbol{Z_U T_U}} + \frac{\boldsymbol{P_R V_R}}{\boldsymbol{Z_R T_R}} = \frac{\boldsymbol{P_F(V_U + V_R + V_V)}}{\boldsymbol{Z_F T_F}} \qquad \textbf{7}$$

Assuming the system is isothermal before and after the expansion and the gas is ideal,

$$\boldsymbol{P_U V_U + P_R V_R = P_F(V_U + V_R + V_V)} \qquad \textbf{8}$$

All values of Equation 8 are known in the volume calibration experiments except for V_U. A volume ratio of the unknown volume to the volume of the reference can be defined as

$$\boldsymbol{\theta_c = \frac{V_U}{V_R}} \qquad \textbf{9}$$

With this, as well as assuming the internal volume of the valve is small relative to the total volume, Equation 3 can be simplified to

$$\boldsymbol{\theta_C = \frac{P_F - P_R}{P_U - P_F}} \qquad \textbf{10}$$

Thus, knowing each of the three pressures in Equation 8 as well as the volume of the reference cylinder allows the volume of any isolated part of the adsorption system to be calculated.

$$\boldsymbol{V_U = V_R * \frac{P_F - P_R}{P_U - P_F}} \qquad \textbf{11}$$

The reference cylinder was filled with water to determine its volume.

Table 5. Known volume of the reference cylinder

Wt R, empty	267.052	g
Wt R, full	316.437	g
Wt water	49.385	g
VCR Vol, Total	1.11	cm^3
Total Vol	50.495	cc

Volume Calibration Procedure: The volume of each subsystem was systematically determined by closing different combinations of valves and restricting helium flow to only certain parts of the overall system. 7 valve combinations, with 5 replicates of each combination, were conducted to determine system volumes. Volumes were determined for the upper manifold, Va, Vb, Vas, and Vbs. The volume of a pneumatic valve was also determined by running an experiment on the same sample system with that valve both opened and closed. Volumes of individual parts were found by taking the difference between subsystems. For example, the volume of Vas only was determined by subtracting the volume of subsystem Va (6, 7, 8, and 9 closed) from the volume of system Vaas (6, 8, and 9 closed). The results of each experiment are shown in Table 6 and the volumes of each subsystem are shown in Table 7.

Table 6. Volume Calibration Data

Upper Manifold (CLOSE 5,6,7,8,9)				
Run	**Pi (bar)**	**P1 (bar)**	**Pf (bar)**	**Volume (calc)**
1	20.56	0	7.47	88.48
2	10.85	2.45	5.52	87.67
3	16.00	6.11	9.71	88.23
4	41.01	9.77	21.09	88.86
5	9.52	1.18	4.22	88.03
			AVG	**88.25**
			ST DEV	**0.45**

Va (CLOSE 6,7,8,9)				
Run	**Pi (bar)**	**P1 (bar)**	**Pf (bar)**	**Volume (calc)**
1	2.96	0.41	1.20	112.50
2	15.7	10.24	11.92	113.61
3	25.23	20.21	21.75	114.11
4	8.71	3.08	4.82	112.89
5	20.45	14.82	16.55	113.83
			AVG	**113.39**
			ST DEV	**0.67**

Vbs (CLOSE 5,7,8,9)				
Run	**Pi (bar)**	**P1 (bar)**	**Pf (bar)**	**Volume (calc)**
1	33.98	38.02	36.83	120.93
2	22.25	26.86	25.54	125.85
3	12.91	18.06	16.6	127.62
4	5.27	10.8	9.21	125.13
5	17.66	21.88	20.67	125.61
			AVG	**125.03**
			ST DEV	**2.48**

Va+Vb+Manifold (CLOSE 7,8) (9 OPEN)				
Run	**Pi (bar)**	**P1 (bar)**	**Pf (bar)**	**Volume (calc)**
1	12.78	1.50	4.48	140.64
2	19.87	3.75	8.01	140.58
3	40.82	9.91	18.04	141.49
4	30.37	6.95	13.15	140.25
5	6.67	1.04	2.53	140.30
			AVG	**140.65**
			ST DEV	**0.50**

Vb (CLOSE 5,7,8,9)				
Run	**Pi (bar)**	**P1 (bar)**	**Pf (bar)**	**Volume (calc)**
1	18.97	21.65	20.81	110.61
2	15.35	18.17	17.32	117.03
3	7.41	10.43	9.49	111.73
4	5.12	8.2	7.25	113.22
5	31.71	36.26	34.88	115.99
			AVG	**113.72**
			ST DEV	**2.74**

Va+Vb+Manifold (CLOSE 7,8) (9 CLOSED)				
Run	**Pi (bar)**	**P1 (bar)**	**Pf (bar)**	**Volume (calc)**
1	13.08	2.10	5.01	140.03
2	19.48	3.77	7.92	140.66
3	39.62	9.50	17.42	141.54
4	29.88	7.37	13.32	140.54
5	6.06	1.17	2.47	139.44
			AVG	**140.44**
			ST DEV	**0.78**

Vas (CLOSE 6,8,9)				
Run	**Pi (bar)**	**P1 (bar)**	**Pf (bar)**	**Volume (calc)**
1	10.71	5.45	6.97	124.24
2	25.34	19.99	21.52	126.07
3	16.50	11.25	12.77	123.91
4	8.13	2.78	4.35	121.57
5	40.35	35.11	36.6	127.08
			AVG	**124.58**
			ST DEV	**2.13**

Table 7. Volumes of system components determined from calibration experiments.

V manifold	88.25	cm^3
Va	25.13	cm^3
Vb	25.46	cm^3
Vas	11.19	cm^3
Vbs	11.31	cm^3

Temperature Calibration

The operating equations for determining the number of observed moles at non-isothermal conditions were corrected by determining a factor τ_A. Essentially the correction factor accounts for the fact that the sample cells and remainder of the system are not at the same temperature. The derivation makes the assumption that V_B and the valve volume V_7 are at a room temperature and that some fraction of the sample cells immersed in the dry ice/acetone bath are maintained at a constant temperature of approximately 195K. The fraction is determined experimentally as detailed below.

The temperature correction factor τ_A is defined as

$$\tau_A = \frac{v_{BBS}^{TC}}{v_{BBS}} = \frac{V_B + V_{BS}\frac{Z_{RT}T_{RT}}{Z_{BS}T_{BS}^{avg}} + V_6}{V_B + V_{BS} + V_6} \qquad \textbf{12}$$

It is the ratio of the temperature corrected reduced volume to the reduced volume of the system when it is entirely at the temperature of the room. Note that it takes into account both the volume of the system above the dry ice/acetone bath V_B as well as below. The non-isothermal reduced volume for the sample cell is corrected by a ratio of the compressibility factor and temperature at room temperature to the compressibility factor and temperature of the cold bath.

Experimentally, the correction parameter τ_A is found by using helium with the sample loaded at the temperature which will be used for the real adsorption experiments. The τ_A parameter is found using the equation below and the full derivation can be found in Chapter 7.

$$P_A^o \frac{V_A}{Z_A R T_{RT}} = \frac{P_A}{Z_{RT} R T_{RT}} V_{AAS} \tau_A \qquad \textbf{13}$$

The RPM3-Zn is degassed by heating under vacuum on the differential pressure adsorption unit at 150°C for 10 hours to desorb any gas in the sample. After this time, the sample is cooled and is ready for the temperature calibration. A dry ice/acetone bath is prepared in a dewar and both sample cells are submerged in the bath. Dry ice is added until it no longer melts and this was taken as the minimum temperature the bath would reach, approximately 195K.

A volume of helium is charged to the evacuated system with valves 7 and 8 closed. The initial charge pressure P_A^o is recorded from the absolute pressure gauge. Next the A and B sides are isolated by closing valves 5, 6, and 9. The volume of V_A is already known from the volume calibration and the compressibility factor of helium is taken to be 1 at room temperature. The dP between the cells is monitored until equilibrium is reached. After the temperature has equilibrated in the system, valves 7 and 8 are simultaneously opened. In order to get a true pressure of P_A after equilibration, valve 6 is opened so that that pressure can be backed solved from the differential and absolute pressure reading. Z_A was calculated using the SRK equation of state and the critical properties for helium. With these values, τ_A was calculated. The process was repeated 3 different times at different charge pressures. The average τ_A was determined to be 1.0232.

Pao	27.35	93.9	29.03	atm
Va	25.13	25.13	25.13	cc
Za	1.011	1.04	1.012	
R	82.057	82.057	82.057	
Trt	298.4	298.4	298.4	K
Pa	18.56	63.122	19.77	atm
Zrt	1.012	1.043	1.013	
Vaas	36.32	36.32	36.32	cc
τA	1.02063	1.032244	1.016988	
Average τA	1.023287			

The Micromeritics ASAP 2020 machine corrects for a temperature gradient between the 'system' and adsorption sample cell in a similar way. Instead of introducing a correction parameter to apply to the reduced volume at room temperature, it directly corrects the 'free space' volume. According to the operating manual, the system uses the equation

$$\boldsymbol{V_f = \frac{V_{SYS} * T_{STD}}{T1} * \left(\frac{P_1}{P_2} - 1\right)} \qquad \textbf{14}$$

where V_f is the free volume, V_{SYS} is the manifold volume, T_{STD} is standard temperature 273.15K, T1 is the system manifold temperature, P_1 is the manifold pressure before helium is dosed to the sample, and P_2 is the manifold pressure after helium is dosed to the sample.

To determine the moles of gas adsorbed the Micromeritics machine uses Equation 15 and Equation 16,

$$\boldsymbol{N_{GAS_I} = N_{GAS_{I-1}} + V_{SYS} * \left(\frac{P_{SYS1_I}}{T_{SYS1_I}} - \frac{P_{SYS2_I}}{T_{SYS2_I}}\right) * \left(\frac{T_{STD}}{P_{STD}}\right)} \qquad \textbf{15}$$

$$\boldsymbol{N_{GAS_I} = N_{ADS_I} - \left(P_{SAM_I} * V_f\right) * \left(\frac{T_{STD}}{P_{STD}}\right)} \qquad \textbf{16}$$

where N_{GASI} is the total amount of gas dosed into the sample tube after the I^{th} dose, $N_{GAS\ I-1}$ is the amount of gas dosed into the tube at the previous dose, P_{SYSI1} and P_{SYSI2} is the system manifold

pressure before and after the I^{th} dose of gas onto the sample, T_{SYSI1} and T_{SYSI1} is the system manifold temperature before and after the I^{th} dose of gas onto the sample, T_{STD} and P_{STD} are standard temperature and pressure, and P_{SAMI} is the sample pressure after equilibrating the I^{th} dose of gas onto the sample [11].

The main differences between the way a commercial piece of equipment, like the Micromeritics ASAP 2020, and this custom differential pressure system calculate moles adsorbed and handle temperature gradients is in the way the "free volume" is calculated. In the operating equation derived for the differential pressure system, the temperature correction τ_A is determined through helium blank experiments and, in the current methodology, is not changed in real time with the actual adsorption experiment. This assumption that τ_A is not changing in the differential pressure experiments has a significant impact on the way the results are calculated and may not be representative of the state of the system for the entire course of the experiment. This will be explored further in Chapter 5.

Chapter 5 Results and Discussion

Experiments were conducted with nitrogen at both 20 bar and 65 bar. Two trials of each experiment were completed and the results are shown in Figure 13 and Figure 14. In between each trial, the adsorbent sample cell was degassed by heating at 150°C for 8 hrs using a heat jacket controlled by a microcontroller. The piping to the sample cell was also wrapped in a heated tape. The sample cells were cooled to room temperature before immersion in the acetone bath to start the next trial. At the conclusion of all N_2 trials the same conditions and procedures were repeated, with helium to serve as the non-adsorbing blank experiment.

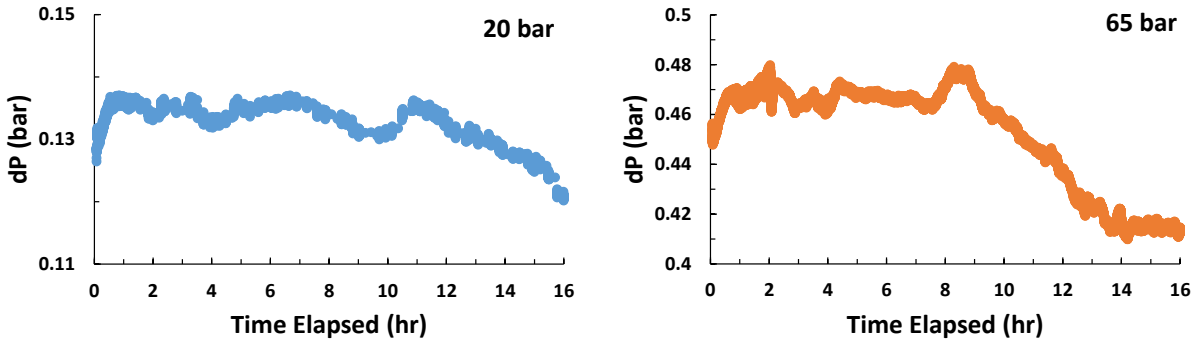

Figure 11. Helium blank experiment at 20 bar (left) and 65 bar (right) vs. dP for the full 16 hour experiment.

As stated in Chapter 3 the purpose of the helium blank experiments was to determine the differential pressure that should be expected for a non-adsorbing gas; it is used to correct the differential pressure of the nitrogen experiments. The differential pressure observed with the helium experiments is the result of system asymmetries, as well as differences in the amount of adsorbent sample and ballast material in cells A and B. In this experiment the dP^{He} may have been more dramatic than expected, as the ballast material mass was not removed and reweighed between this work and previous work. Figure 11 shows the dP observed for the entire 16 hour

experiment. The fluctuation in dP with time is particularly concerning, as the goal of this experiment was to have a steady and constant helium differential pressure value with which to use in Equation 4 to determine the moles of nitrogen adsorbed. In the 20 bar experiment the differential pressure fluctuated between 0.12 and 0.14 bar, with a mean value of approximately 0.13. This is not concerning, as the tolerance of the instrument is 0.01 bar. In the 65 bar experiment, the differential pressure fluctuated between 0.41 and 0.48 bar over the course of 16 hours. This is well outside of the tolerance of the instrument and it would not be appropriate to determine a helium differential pressure from the average value of this data set. One reason for this fluctuation is hypothesized to be due to the temperature cycling in the lab over the course of 16 hours. Both experiments were started around the same time of day and the same relative trend is observed in both experiments, though not as dramatic in the 20 bar experiment. The second reason this fluctuation may have been observed was the decreasing level of acetone in the dewar with time. The fluctuation may have been more severe at high pressure due to the larger measurement being taken or simply less control over the temperature of the bath This idea is developed further later.

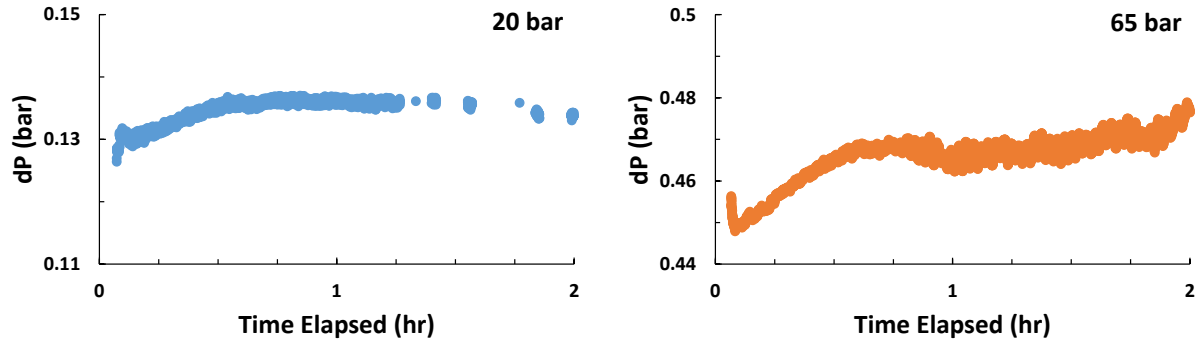

Figure 12. Helium blank experiments at 20 bar (left) and 65 bar (right) vs. dP for only the first two hours where a steady state appears to be reached.

Figure 12 shows just the first 2 hours of data for the helium experiments. In both experiments steady state is not reached until approximately 30 minutes. As helium is non-adsorbing, this suggests that contamination may have been introduced into the RPM3-Zn sample. This may include acetone from the temperature bath that the cells are immersed in or remaining from the material synthesis. In the future, this could be checked by monitoring the exhaust of the vacuum pump with a mass spectrometer for evidence of acetone leaving the system during the degas procedure. The mean dP value between 0.5 hrs and 2 hrs was used for all future calculations.

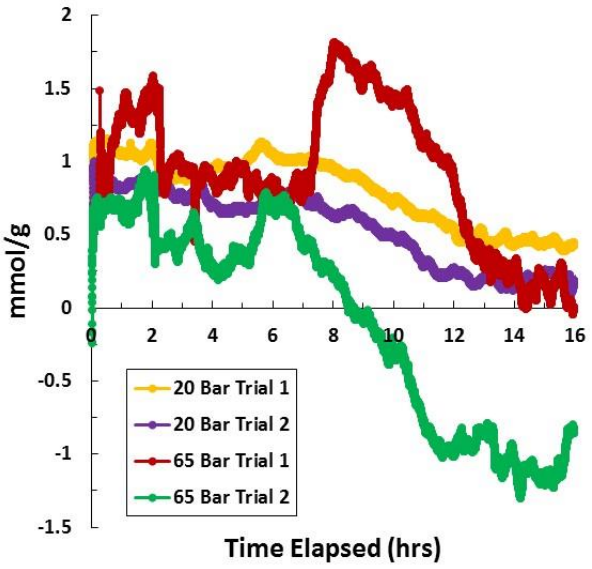

Figure 13. All nitrogen experiment trials in units of mmol of nitrogen adsorbed per grams of sample vs elapsed time.

The moles of N_2 adsorbed vs. time was calculated using Equation 4 outlined in Chapter 3. The LabView program records dP vs. time and from the dP recorded the mmoles/g vs. time could be determined. Speaking generally about the trends in the 4 nitrogen trials, all follow a similar trajectory with mmol/g adsorbed vs. time. The moles adsorbed initially spikes as high pressure nitrogen rushes into the vacuum that the sample cells are under. The moles adsorbed

reaches a steady state at an upper bound and maintains for approximately 6 hours before it slowly begins to rise. After approximately 8 hours the differential pressure decreases linearly until it again reaches a steady state at a differential pressure lower than the first. This steady state is then maintained for the duration of the experiment.

As alluded to before, the change in moles adsorbed are thought to be a function of the decreasing level of acetone during the course of the experiment and fluctuations in the temperature of the room which led to fluctuations in the temperature of the manifold. Acetone was initially filled to 1 inch below the lip of the dewar. This was enough to completely cover both sample cells A and B, as well as about one inch of the metal piping. Neither the acetone or dry ice were replenished during the course of the 16 hours. At the conclusion of the experiment the acetone level was, at a minimum 2 inches below the lip of the dewar and in some cases as low as 3 inches. As a note, the decreasing level is thought to be due to the sublimation of the dry ice and not evaporation of acetone.

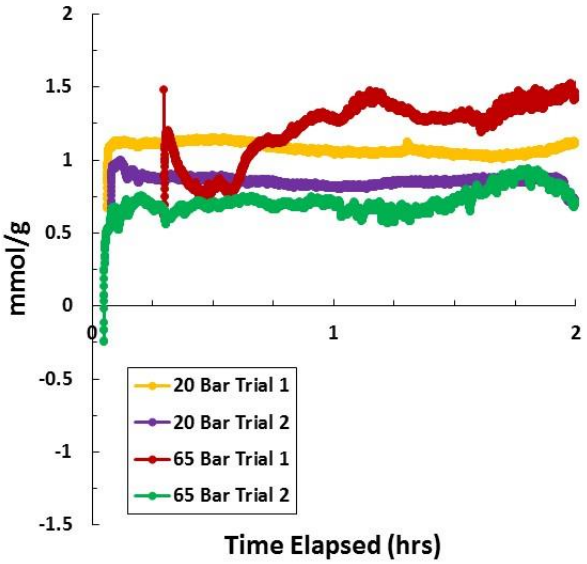

Figure 14. Truncated results for the nitrogen adsorption experiments, showing only the first 2 hours of data.

The error associated with the full 16 hours of data renders any extended time conclusions about the adsorption kinetics of the experiment inappropriate. However, data from all 4 trials shows that moles adsorbed reaches a steady state in the same 2 hour time frame as the helium experiments. The average mmol/g was taken for each trial over these 2 hours and is shown below.

Table 8. Average mmol/g over the first 2 hours of the experiments.

20 Bar Trial 1	0.540	mmol/g
20 Bar Trial 2	0.854	mmol/g
65 Bar Trial 1	1.222	mmol/g
65 Bar Trial 2	0.711	mmol/g

One of the most important goals of this experiment was to compare the results of this experiment to data collected at the same experimental conditions on the Hiden gas sorption analyzer. This data in presented in Figure 6. Using nitrogen at 20 bar and 195K with RPM3-Zn, the amount of gas adsorbed was approximately 1.8 mmol/g in that experiment[8]. As shown in Table 8, at the same experimental conditions 0.540 mmol/g and 0.854 mmol/g were observed. While the same result was not seen exactly, considering the error in the experimental set up seen previously this is within a reasonable magnitude. It should also be noted that even in tripling the nitrogen pressure, nearly the same amount of gas was adsorbed. This, too, it not particularly surprising because Figure 6 shows that after approximately 14 bar the moles of adsorption plateaus.

The most important visual observation about the experimental set up during the course of the 16 hr experiment was that, despite being wrapped in an insulated bag, the acetone level in the dewar dropped dramatically during the course of the experiment. Acetone and dry ice were not replenished or altered during the course of the experiment. At the end of the 16 hours, in most

cases the acetone level had dropped between one and two inches from where it started. There was still dry ice remaining in the dewar so the concern is not the temperature of the bath was changing, but that the τ_A parameter was varying with time. Future experimentation must focus around the temperature dependence of τ_A as this will help to clarify the impact that the dropping level of the acetone bath has on the differential pressure and by extension the moles of gas adsorbed.

Returning to the definition of τ_A and assuming the level of acetone varied enough to affect the ratio of "warm space" to "cold space" it would be expected that the "cold space" volume would decrease and thus the "cold space" pressure would increase. This would consequently mean that τ_A should be decreasing with time and, when plugging into the operating equation, the moles of nitrogen adsorption should also be decreasing with time. Following this line of logic and assumption, the moles of nitrogen adsorbed towards the end of the experiment may have been underestimates. This again underscores the importantance of determining the functional dependence of acetone volume, or time, on τ_A.

Future Work

It is important to note that there are many sub-calculations and experiments that contributed to reaching these final numbers. They are subject to the results of the pressure calibration, volume calibration, temperature calibration, helium blank experiments, and determination of the compressibility factor at these conditions. They are limited by the accuracy of the pressure transducers, assumption that the system does not have appreciable leaks, and fluctuation in the temperature and level of the acetone/dry ice bath. Any number of these items could have contributed to the results reported; intuitively, there should not have been more helium adsorbed in the blank experiment than nitrogen adsorbed in the real experiment at any

point. This is likely a result of a contaminated sample, whether that mean the sample was not entirely degassed before the previous experiment or that there was solvent remaining in the sample.

Temperature stability of both the lab and of the bath appear to be the biggest reason that such dramatic fluctuations of absorbance were seen with time. While starting experiments at the same time of day allowed the system to experience the same temperature cycling of the room, in the future efforts should be made to maintain the lab at the same temperature over the course of the day. It would be helpful to do longer experiments, for perhaps 48 or 72 hours, to see if the dP vs. time does indeed cycle with the time of day. Additionally, it is very important to keep the temperature bath at the same level. The decreasing level of acetone in the bath changed the temperature profile of the system and this likely caused the τ_A parameter to change over the course of the experiment. This is problematic, as a constant value was used in subsequent calculations. It may be necessary to refill the bath every 4-6 hours, as these experiments showed the strong dependence of moles adsorbed on temperature.

It is also important to reevaluate how the helium blank experiment is run. It was run at 195K for consistency with the temperature used in the nitrogen experiments. This work, however, showed that the differential pressure when helium is used is highly temperature sensitive. Comparing the dP observed at room temperature with the dP observed for the initial 2 hours at 195K may be beneficial. If they are the same it may not be necessary to run the blank experiments at 195K. Helium, in theory, is non-adsorbing and so it is not unreasonable to expect they should be a similar value. The dP^{He} was a constant value used for all subsequent calculations so it is important to conduct future experiments on why a fluctuation with time was observed.

Lastly, it may be important to reevaluate the operating equation used for determining moles adsorbed in these experiments. Equation 6 is dependent on the fact that dP^{He} and τ_A are constant with time. If a procedure cannot be developed on this equipment to ensure these parameters are reliable and indeed constant, their dependence with temperature must also be determined so that the moles of adsorbed gas can be calculated accurately.

Chapter 6 Conclusion

The results of this experiment answer the question "what is the expected nitrogen adsorption at 195K when using an uncontrolled temperature bath for RPM3-ZN at various pressures?" Acknowledging that the results depends on the result of many prework experiments and calculations, the moles of adsorbed at 20 and 65 bar do not differ that drastically. This was to be expected, as previous work showed a plateau in adsorption amount around 14 bar at 195K.

These results raise the question of at what threshold does the pressure applied become irrelevant such that the material has already adsorbed the maximum amount of N_2 that it can based on the structural constraints and properties of that material. These experiments have brought to the light the high sensitivity of results to both the temperature of the room and level of the acetone bath. While the results of this work were within 1 mmol/g of the results of the IGA, where temperature is better controlled, more work must be done on this differential pressure system around temperature control before results can be considered reliable.

Chapter 7 Derivation

Derivation of τ_A Parameter[8]

Define the system by,

$$P_A^o v_A = P_A^o \int_6^8 \frac{A_i(x)dx}{Z_i(x,T,P)RT_i(x)} = P_A v_{AAS} = \int^z \frac{A_i(x)dx}{Z_i(x,T,P)RT_i(x)}$$

This can be written,

$$P_A^o v_A = P_A^o \frac{V_B}{Z_B RT_B^{avg}} = P^A v_{AAS} = P_A \frac{V_{AAS}}{Z_{AAS} RT_{AAS}^{avg}} = P^A \left[\frac{V_A}{Z_A RT_A^{avg}} + \frac{V_{AS}}{Z_{AS} RT_{AS}^{avg}} + \frac{V_6}{Z_6 RT_6^{avg}}\right]$$

Assuming the upper volume are maintained at a constant temperature,

$$P_A^o \frac{V_A}{Z_A RT_{RT}} = \frac{P_A}{Z_{RT} RT_{RT}} \left[V_A + V_{AS} \frac{Z_{RT} T_{RT}}{Z_{AS} T_{AS}^{avg}} + V_6\right] = \frac{P_A}{Z_{RT} RT_{RT}} V_{AAS}^{TC} = P_A v_{AAS}^{TC}$$

Defining the temperature corrected volume,

$$v_{AAS}^{TC} = \frac{V_{AAS}^{TC}}{Z_{RT} RT_{RT}} = \frac{V_A + V_{AS} \frac{Z_{RT} T_{RT}}{Z_{AS} T_{AS}^{avg}} + V_6}{Z_{RT} RT_{RT}}$$

Defining the temperature correction parameter,

$$\tau_A = \frac{v_{AAS}^{TC}}{v_{AAS}} = \frac{V_A + V_{AS} \frac{Z_{RT} T_{RT}}{Z_{AS} T_{AS}^{avg}} + V_6}{V_A + V_{AS} + V_6}$$

Combining equations,

$$P_A^o \frac{V_A}{Z_A RT_{RT}} = \frac{P_A}{Z_{RT} RT_{RT}} V_{AAS} \tau_A$$

Bibliography

[1] Atkins, T.; Escudier, M. Oxford Dictionary of Mechanical Engineering; 2013.

[2] Suresh, B.; Gubler, R.; Yamaguchi, Y.; He, H. *Chemical Economics Handbook Air Separation Gases*; rep.; 2013; pp. 1–360.

[3] Sircar, S. Pressure Swing Adsorption. *Ind. Eng. Chem. Res.* 2002, *41*, 1389–1392.

[4] Li, P.; Chen, J.; Feng, W.; Wang, X. Adsorption Separation of CO2 and N2 on MIL-101 Metal-Organic Framework and Activated Carbon. *Journal of the Iranian Chemical Society*. 2013.

[5] Burtch, N.; Jasuja, H.; Walton, K. Water Stability and Adsorption in Metal-Organic Frameworks. *Chemical Reviews*. 2014, 10575–10612.

[6] Lan, A. RPM3: A Multifunctional Microporous MOF And Recyclable Framework and High H2 Binding Energy. *Inorganic Chemistry*. 7165–7173.

[7] Lueking, A.; Li, J. *Probing Oxygen Selectivity in a Flexible Metal-Organic Framework Using In Situ Spectroscopy*; rep.

[8] Sircar, S.; Wang, C.-Y.; Lueking, A. Design Of High Pressure Differential Volumetric Adsorption Measurements with Increased Accuracy. *Adsorption*. 2013, *19*.

[9] Oxy-Combustion. US Department of Energy.

[10] Tanaka, D. Kinetic Gate-Opening Process In a Flexible Porous Coordination Polymer. *Coordination Polymers*. 2007, 3978–3982.

[11] Micromeritics User Manual.

[12] Coolings Baths. *UC Davis ChemWiki*. UC Davis.

ACADEMIC VITA

Andrew D. Belnick
drew.belnick@gmail.com

EDUCATION The Pennsylvania State University – University Park, PA Class of 2016
Schreyer Honors College
Bachelor of Science, Chemical Engineering
Engineering Leadership Development Minor

EXPERIENCE

W.L. Gore & Associates Inc. – Elkton, MD *Summer 2015*
Technical Intern – Fabrics

- Evaluated the hole detection test methods used on Gore Tex and identified inherent properties of the tests that could bias a particular waterproof technology
- Developed and executed a multi-tiered experimental plan that isolated and challenged each potential bias, material property, and damage type individually
- Created a plan to address why unexpected trends were observed and their implication for future testing within the division
- Partnered with Associates at Gore Germany to complete testing on equipment not available in the US
- Worked effectively in the lattice culture, which required a self-driven and self-sufficient work style

W.L. Gore & Associates Inc. – Elkton, MD *Summer 2014*
Technical Intern – PharmBio

- Qualified water entry pressure test equipment and designed a validation test method in the quality system
- Explored and characterized taper tension/torque functionality on roll goods narrow slitting equipment to better understand the machine's capabilities
- Supported the PharmBio industry, which involved understanding and working within a regulated industry quality system, using clean concepts, and functioning in a clean room manufacturing environment

Bimax Inc. – Glen Rock, PA *Summer 2013*
Student Intern

- Acted as principle researcher in a HEMA purification project to increase monthly output by 20 – 40 drums
- Connected the lab and plant floor by writing batch records and material balances for five new products
- Participated in Hazardous Operation and Failure Mode and Effect Analysis meetings with the goal of ensuring OSHA compliance and improving the quality of products

PROJECTS

Bay Oil Distillation Project – University Park, PA *Spring 2014*

- Collaborated with a cross-national team of students from Penn State and Corvinus University in Budapest, Hungary to analyze the bay oil distillation process used in remote parts of Dominica
- Made recommendations that would yield natural resource savings of 3600 trees per year

Moringa Harvesting Project – University Park, PA *Fall 2013*

- Worked with a team of students to fund, design, and build a prototype for a machine that would reduce the time required to harvest moringa in Sub-Saharan Africa

Eagle Scout Project and Award – York, PA *February 2012*

- Supervised and directed a team of 10 scouts in assembling a pergola and two benches for a local school

LEADERSHIP

Vice President, Penn State Blue Band *2014 - Present*

- Coordinated volunteer, scholastic assistance, public relations, and social opportunities for the band
- Served as the liaison for communication between the director team and student leadership team

Engineering Ambassador, Penn State College of Engineering *2014 – Present*

- Trained in advanced written and oral engineering communication
- Represented the Penn State College of Engineering on campus tours to prospective students and families
- Inspired middle and high school students to pursue STEM careers through lessons and activities

Dancer Relations Committee Member, Penn State Dance Marathon *2015 – 2016*

- Provided morale to a THON dancer for 46 hours so they could be there for the Four Diamonds kids

Treasurer, Penn State Circle K *2013 – 2015*

- Managed a $4000 budget which involved allocating money to student volunteer projects and charities

HONORS

McWhirter Student Excellence Scholarship in Chemical Engineering *2012 – Present*
President's Freshman Award for Academic Excellence *2012-2013*